

# Spin-Spin and Spin-Orbit Interactions in Strongly Coupled Gauge Theories

Edward V. Shuryak and Ismail Zahed

*Department of Physics and Astronomy*

*State University of New York, Stony Brook, NY 11794-3800*

(October 18, 2018)

We evaluate the spin-orbit and spin-spin interaction between two fermions in strongly coupled gauge theories in their Coulomb phase. We use the quasi-instantaneous character of Coulomb's law at strong coupling to resum a class of ladder diagrams. For  $\mathcal{N} = 4$  SYM we derive both weak and strong coupling limits of the the spin-orbit and spin-spin interactions, and find that in the latter case these interactions are subleading corrections and do not seriously affect the deeply bound Coulomb states with large angular momentum, pointed out in our previous paper. The results are important for understanding of the regime of intermediate coupling, which is the case for QCD somewhat above the chiral transition temperature.

**Introduction.** QCD at temperatures  $T = (1 - 3)T_c$  is in a chirally restored but relatively strongly coupled Coulomb phase. Although it is known for long time that some aspects of this regime are nonperturbative (see [1,2] and references therein), and although explicit evaluation of perturbative series for thermodynamical quantities are not convergent in this domain, till recent times one have mostly relied on perturbative ideas for signal assessment at RHIC. Recently, we have suggested [3] that this region of temperatures supports  $\bar{q}q$  (light and heavy) and  $gg$  Coulomb bound states, enhanced due to running of the coupling to smaller momentum scale as compared to the vacuum. Charmed and even light flavor mesonic states beyond the chiral restoration transition have been also observed on the lattice. In [3] we further suggested that the scattering cross section peak near the lines of zero binding energy, and reach large values, explaining why the QGP at RHIC behaves hydrodynamically.

The nonperturbative character of the Coulomb phase can be further investigated in  $\mathcal{N} = 4$  SYM in the Maldacena limit [4], at parametrically strong coupling  $\lambda = g^2 N \gg 1$  (where  $N$  is the number of colors) and finite temperature  $T$ . In particular, the potential between two static Coulomb charges is found to obey a modified Coulomb's law [4,5].  $\mathcal{N} = 4$  SYM at finite temperature and in strong coupling is similar to QCD across the chiral restoring temperature  $T_c$ . We recall, that a number of pertinent issues have been addressed in strongly coupled  $\mathcal{N} = 4$  SYM, such as small angle scattering [6,7], large angle scattering [8], the free energy [9], the electric Debye screening [10], the viscosity [11], and real-time correlators [12].

The puzzling aspect of all the finite temperature results is that they are independent of the strong coupling constant  $\lambda = g^2 N_c$ , even though the (modified) Coulomb interaction is proportional to  $\sqrt{\lambda}$ . The naive quasiparticles carry thermal Coulomb energies of order  $\sqrt{\lambda}T$ , making them way too heavy to be thermally excited in the Coulomb phase. Hence, what is the finite-T matter in the strongly coupled Coulomb phase made of? The answer to this question was suggested in [3], where it was

pointed out that in the strong coupling regime, there exists about a constant density of deeply bound composite states of mass  $m \approx T$  at large  $\lambda$ . These composites are made of two quasiparticles which rotate with a large angular momentum  $l \approx \sqrt{\lambda}$ , compensating the supercritical Coulomb force.

The present paper addresses the following issue. In [3] the spectrum of the composites was limited to the simplest case of spinless scalars obeying the Klein-Gordon equation. The cases of composites made of two fermions and/or gluons were only discussed qualitatively. One may wonder what exactly is the role of the spin-spin and spin-orbit interactions in these highly relativistic states, especially since the orbital momentum is parametrically large. In this letter we answer this question by extending the arguments of [3] to the spin-spin and spin-orbit interactions at strong coupling: we will show that these forces are subleading in the strong coupling limit.

In principle, this question can be exactly addressed using the AdS/CFT correspondence by evaluating the averages of pertinent supersymmetric Wilson lines for spinning and moving (non-static) particles along externally chosen paths. Such approach should yield exact answers with exact coefficients. Alternatively, one can also obtain parametrically correct answers (without exact coefficients) using the resummation of ladder diagrams. This was first demonstrated for the modified Coulomb's law in [13], see also the discussion of the higher order and screening effects in [3]. The key physics idea is that in the strong coupling regime gauge (scalar) exchanges between two charges separated by a distance  $L$  takes place during a short time  $L/\lambda^{1/4}$ , in contrast to the weak coupling regime where it is of order  $L$ .

After briefly recalling the derivation of the modified Coulomb's law in  $\mathcal{N} = 4$  SYM using the ladder resummation, we introduce the correlator of two "spinning" fermionic lines. In the relativistic case the mass in the magnetic moment is substituted by the (relativistic) kinetic energy of the external particle on its classical orbit. We use a ladder resummation both in weak and strong coupling to derive the spin induced interactions between

spin 1/2 particles. In weak coupling, we reproduce the familiar Breit-Fermi interaction, while in strong coupling a novel spin-induced interaction is derived. The spin-induced interactions are used to qualitatively assess the spin splittings in QCD across the chiral restoring temperature.

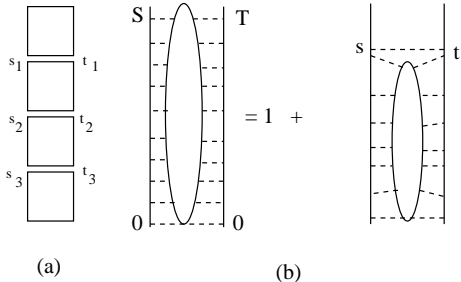


FIG. 1. (a) The color structure of ladder diagrams in the large- $N_c$  limit: each square is a different color trace, bringing the factor  $N_c$ . The time goes vertically, and the planarity condition enforces strict time ordering,  $s_1 > s_2 > s_3, \dots$ ,  $t_1 > t_2 > t_3, \dots$ . (b) Schematic representation of the Bethe-Salpeter equation (1) summing ladders.

**The modified Coulomb's law.** In the limit where the number of colors  $N_c$  is large and the coupling  $\lambda = g^2 N_c$  is large as well, charges in  $\mathcal{N} = 4$  SYM communicate with quasi-instantaneous and nearly abelian interactions. This legitimates the use of ladder diagrams to understand the nature of the strong interaction between heavy [13] and light charges.

The quasi-instantaneous potential between two charges at a distance  $L$ , can be obtained by resumming the ladder diagrams displayed in Fig. 1. The pertinent Bethe-Salpeter kernel is solution to the integral equation

$$\Gamma(\mathcal{S}, \mathcal{T}) = 1 + \frac{\lambda}{4\pi^2} \int_0^{\mathcal{S}} ds \int_0^{\mathcal{T}} dt \frac{1}{(s-t)^2 + L^2} \Gamma(s, t). \quad (1)$$

The first factor under the integral is the (Euclidean) propagator for one extra gluon/scalar added to the ladder. The kernel satisfies the boundary condition  $\Gamma(\mathcal{S}, 0) = \Gamma(0, \mathcal{T}) = 1$ . when the equation is solved, the ladder-generated potential follows from

$$V_{\text{lad}}(L) = - \lim_{T \rightarrow +\infty} \frac{1}{T} \Gamma(\mathcal{T}, \mathcal{T}), \quad (2)$$

In weak coupling  $\Gamma \approx 1$  and the integral on the rhs is easily taken, resulting in

$$\Gamma(\mathcal{S}, \mathcal{T}) \approx 1 + \frac{\lambda}{8\pi} \frac{\mathcal{S} + \mathcal{T}}{L} \quad (3)$$

which results into the standard Coulomb's law. Note that in this case the typical relative time difference between emission and absorption of a quantum  $|t - s| \approx L$ , so one can say that virtual quanta travel at a speed  $v \approx 1$ . In strong coupling, the kernel can be obtained using the

method outlined in [13]. For  $x = (\mathcal{S} - \mathcal{T})/L$  and  $y = (\mathcal{S} + \mathcal{T})/L$ , the result for large times  $\mathcal{S} \approx \mathcal{T}$  that is small  $x$  and large  $y$  is

$$\Gamma(x, y) \approx \mathbf{C}_0 e^{-\sqrt{\lambda} x^2 / 4\pi} e^{\sqrt{\lambda} y / 2\pi}. \quad (4)$$

From (2) it follows that in the strong coupling limit the ladder generated potential is

$$V_{\text{lad}}(L) = - \frac{\sqrt{\lambda} / \pi}{L} \quad (5)$$

which has the same parametric form as the one derived from the AdS/CFT correspondence [4,5] except for the overall coefficient. The discrepancy is due to the left out higher-order diagrams discussed in [3].

For physics it is important to stress again that in the strong coupling limit  $\lambda = g^2 N \gg 1$ , the color charges communicate on short time of order  $L/\lambda^{1/4}$  within which the exchange is nearly Abelian. This allows the use of a potential description *even* for relativistically moving charges [3]. So the two particle relativistic problem is emmenable to a bound state problem with a potential at strong coupling.

**Non-static Wilson lines with spin.** To investigate the spin effects on the form of the potential inherited by the resummation of the ladders, we note that the basic correlator between say two relativistic spin  $\frac{1}{2}$  particles follows from the generic correlation function

$$\begin{aligned} \mathbf{C}(\mathcal{T}) = & \left\langle \text{Tr} \mathbf{P} \exp \left( g \int_0^{\mathcal{T}} ds_1 (i \dot{x}_1 \cdot A(x_1) + \frac{1}{4} \sigma_{1\mu\nu} F_{\mu\nu}(x_1)) \right) \right. \\ & \times \exp \left( -g \int_0^{\mathcal{T}} ds_2 (i \dot{x}_2 \cdot A(x_2) + \frac{1}{4} \sigma_{2\mu\nu} F_{\mu\nu}(x_2)) \right) \left. \right\rangle, \quad (6) \end{aligned}$$

with *fixed* external paths. The new spin-dependent additions are the  $\sigma_{1,2}$  terms acting on the spinor indices of both fermionic lines. The path ordering  $\mathbf{P}$  and the trace is over spin and color. The quantum propagator follows from the integration over the external paths  $x_{1,2}$  and the affine time  $\mathcal{T}$ . Gauge invariance is enforced for trajectories with identical end-points  $x_1 = x_2$  at  $s = 0, \mathcal{T}$ . The averaging is over the pertinent gauge field measure.

Supersymmetric spinning lines can be also discussed, but we will not do it here. Since our spinning lines are just external probes rather than part of the underlying gauge theory, their color charges can be chosen at will, e.g. in the fundamental representation. We will also ignore the scalar exchanges, so the correlator is not even supersymmetric. Thus it has divergent self-energy corrections, which however drop out of the interaction potential which we will be calculating below. We further note that the two spinors are chosen to move along the *fixed* external paths, which we can select at will to get the potential we need. The quantum correlator for spin 1/2

follows from (6) by integrating over the external paths  $x_{1,2}$ , which will not be discussed below.

The (diffeomorphic) time integration in (6) is over the affine time  $s$  which has dimensions of inverse mass square. If one uses the laboratory time  $t$  in (6), a relativistic gamma factor of the particle (due to Lorentz invariance) appears, and so  $S = m \int dt \sqrt{1 - \dot{x}^2}$  (in Minkowski notations). Starting with the action of a free particle with affine time  $s$

$$\mathbf{S} = \int_0^T ds \frac{1}{2} (\dot{x}^2 + m^2) \quad (7)$$

one may rewrite it in terms of the conventional time  $t$  using additional parameter  $\mu = dt/ds$

$$\mathbf{S} = \int_0^T dt \left( \frac{\mu}{2} (1 + \dot{x}^2) + \frac{m^2}{2\mu} \right) \quad (8)$$

Note that  $\mu$  in general depends on the particular trajectory. For a free particle it can be set by extremizing the action over  $\mu$  (8) [14], with the result

$$\mu = \frac{m}{\sqrt{1 + \dot{x}^2}} = \gamma m, \quad (9)$$

which is just the relativistic energy of a free particle, since the relativistic momentum in Euclidean space is  $\vec{p} = i\gamma m\dot{x}$ .

In terms of the physical time, the correlation function (6) now reads

$$\begin{aligned} \mathbf{C}(T) = & \left\langle \text{Tr} \mathbf{P} \exp \left( g \int_0^T dt_1 (i \dot{x}_1 \cdot A(x_1) + \frac{1}{4\mu} \sigma_{1\mu\nu} F_{\mu\nu}(x_1)) \right) \right. \\ & \left. \times \exp \left( -g \int_0^T dt_2 (i \dot{x}_2 \cdot A(x_2) + \frac{1}{4\mu} \sigma_{2\mu\nu} F_{\mu\nu}(x_2)) \right) \right\rangle. \end{aligned} \quad (10)$$

In the chiral basis, the spin term reads

$$\frac{g}{4\mu} \sigma_{\mu\nu} F_{\mu\nu} = \frac{g}{2\mu} \vec{\sigma} \cdot (\vec{B} \mathbf{1}_+ - \vec{E} \mathbf{1}_-) \quad (11)$$

with  $\mathbf{1}_\pm = \text{diag}(1, \pm 1)$ . We note that the positive parity of the electric field is flipped by the chirality matrix  $\mathbf{1}_-$ . The spin-coupling to the magnetic field occurs with the correct magnetic moment. The spin-coupling to the electric field is purely imaginary for physical electric fields\*. This point is particularly important in deriving the spin induced interactions, since the electric parts

---

\*Note that it is real for virtual vacuum fields such as instantons.

generate mostly phases that drop from the positive correlation function (10).

In strong coupling the ladder approximation maybe used to assess the nature of the spin forces. For that, the driving kernel is given by the *real parts* of the expectation value

$$\begin{aligned} & \left\langle \left( g (i \dot{x}_1 \cdot A(x_1) + \frac{1}{2\mu} \vec{\sigma}_1 \cdot \vec{B}(x_1)) \right) \right. \\ & \left. \times \left( -g (i \dot{x}_2 \cdot A(x_2) + \frac{1}{2\mu} \vec{\sigma}_2 \cdot \vec{B}(x_2)) \right) \right\rangle, \end{aligned} \quad (12)$$

where the imaginary contributions through the electric field have been dropped. Again the Coulomb kernel arises from the  $AA$  correlator in the form

$$\frac{g^2 C_A}{4\pi^2} \frac{1 + \dot{x}_1 \cdot \dot{x}_2}{(t_1 - t_2)^2 + (\vec{x}_1 - \vec{x}_2)^2} \quad (13)$$

with the Casimir  $C_A = N/2$  in large  $N$ . Note that the velocity dependent part translates in Minkowski space to  $(1 - \vec{v}_1 \cdot \vec{v}_2)$  which is the expected correction to Coulomb's law from Ampere's law as induced by charge motion. This contribution adds for particle-antiparticle or particle-hole, and subtracts otherwise in relativistic bound states. For instance, for relativistic particle-antiparticle states  $v_1 = -v_2$ , twicing the Coulomb interaction. At asymptotic temperature Ampere's induced interaction can still be used space-like to bind in the dimensionally reduced theory [15].

**Spin-dependent contributions.** The spin-orbit contribution follows from the  $AB$  term in the form

$$\left\langle \left( i g \dot{x}_1 \cdot \vec{A}(x_1) \right) \left( \frac{-g}{2\mu} \vec{\sigma}_2 \cdot \vec{B}(x_2) \right) \right\rangle + 1 \leftrightarrow 2 \quad (14)$$

Thus

$$-\frac{g^2 C_A}{4\mu^2} (\vec{\sigma}_2 \cdot (\vec{x}_{12} \times \vec{p}_1) + \vec{\sigma}_1 \cdot (\vec{x}_{21} \times \vec{p}_2)) \frac{1}{\pi^2 x^4} \quad (15)$$

where again we have used  $\vec{p} = i\gamma m\dot{x}$ .

The spin-spin contribution follows from the  $BB$  term in the form

$$-\frac{g^2}{4\mu^2} \sigma_{1i} \sigma_{2j} \left\langle B_i(x_1) B_j(x_2) \right\rangle. \quad (16)$$

The result is

$$\frac{g^2 C_A}{4\mu^2} \left( \vec{\sigma}_1 \cdot \vec{\sigma}_2 \nabla^2 - \vec{\sigma}_1 \cdot \vec{\nabla} \vec{\sigma}_2 \cdot \vec{\nabla} \right) \frac{1}{4\pi^2 x^2}. \quad (17)$$

The spinning ladder diagrams can be generated in the same way as the non-spinning ones described above. In Feynman gauge, the driving kernel in (1) is now

$$\begin{aligned}
& + \frac{\lambda}{8\pi^2 x^2} \left( 1 - \frac{\vec{p}_1 \cdot \vec{p}_2}{\mu^2} \right) \\
& + \frac{\lambda}{8\pi^2 x^4} \frac{1}{\mu^2} (\vec{\sigma}_2 \cdot (\vec{x}_{21} \times \vec{p}_1) + 1 \leftrightarrow 2) \\
& + \frac{\lambda}{32\pi^2 \mu^2} \left( \vec{\sigma}_1 \cdot \vec{\sigma}_2 \nabla^2 - \vec{\sigma}_1 \cdot \vec{\nabla} \vec{\sigma}_2 \cdot \vec{\nabla} \right) \frac{1}{x^2} \quad (18)
\end{aligned}$$

Note that the spin-independent Coulomb term is 1/2 its value in (1) since there is no scalar exchange between the non-supersymmetric external lines in (6).

**Spin-orbit from Thomas precession.** The spin-orbit term induced by Thomas precession is not present in our analysis of (6). For non-accelerating paths, this effect is not even visible. To see it, we note that the spin precess along the trajectory with a rate given by the spin factor [17]

$$\mathbf{P} \exp \left( -i \int_0^\tau d\tau \frac{1}{2} \sigma_{\mu\nu} \dot{x}_\mu \dot{x}_\nu \right), \quad (19)$$

with  $\tau$  the affine proper time with dimensions one over mass. For a non-accelerating external trajectory, this effect is not visible. For a particle in an external field, the 4-acceleration is given by the Lorentz force in proper time

$$m \dot{x}_\nu = g F_{\nu\sigma} \dot{x}_\sigma. \quad (20)$$

Inserting (20) in (19) and using  $\langle \vec{E} \rangle = -i \vec{\nabla} V_E$  for two static charges, it follows that (19) generates

$$-\frac{g^2 C_A}{4\mu^2} ((\vec{\sigma}_1 \times \vec{p}_1) \cdot \vec{\nabla} V_E(\mathbf{x}) + 1 \leftrightarrow 2) \quad (21)$$

which is the standard Thomas contribution (after the 1/2 correction in the energy due to the accelerating frame). This result holds for both weak and strong coupling, with  $V_E(\mathbf{x})$  the pertinent Coulomb potential in strong coupling.

**Potentials in weak coupling.** In weak coupling  $\lambda \ll 1$ , and the standard form of the Coulomb and spin interactions can be obtained by setting  $x^2 = t^2 + \vec{x}_{12}^2$  and integrating over the time  $t$ . The answer is readily found to be

$$\begin{aligned}
\mathbf{V}_{12}(\mathbf{x}) &= -\frac{\lambda}{8\pi |\mathbf{x}|} \left( 1 - \frac{\vec{p}_1 \cdot \vec{p}_2}{\mu^2} \right) \\
& - \frac{\lambda}{16\pi |\mathbf{x}|^3} \frac{1}{\mu^2} (\vec{\sigma}_2 \cdot (\vec{x}_{21} \times \vec{p}_1) + 1 \leftrightarrow 2) \\
& + \frac{\lambda}{32\pi |\mathbf{x}|^3} \frac{1}{\mu^2} \left( \frac{2|\mathbf{x}|^3}{3} \vec{\sigma}_1 \cdot \vec{\sigma}_2 4\pi \delta(\mathbf{x}) + 3\sigma_{T12} \right) \quad (22)
\end{aligned}$$

where we have defined the tensor interaction

$$\sigma_{T12} = \vec{\sigma}_1 \cdot \hat{\mathbf{x}}_{12} \vec{\sigma}_2 \cdot \hat{\mathbf{x}}_{12} - \frac{1}{3} \vec{\sigma}_1 \cdot \vec{\sigma}_2.$$

The presence of  $\mu$  makes the potential non-local in the relativistic limit, since  $\mu$  is determined by the Coulomb trajectory.

The result (22) is the standard Breit-Fermi interaction, modulo the Thomas term as discussed above. For S-states, the induced interaction is

$$\begin{aligned}
\mathbf{V}_{\text{ladd}12}^{L=0}(\mathbf{x}) &= -\frac{\lambda}{8\pi |\mathbf{x}|} \left( 1 - \frac{\vec{p}_1 \cdot \vec{p}_2}{\mu^2} \right) \\
& + \frac{\lambda}{3\mu^2} \vec{S}_1 \cdot \vec{S}_2 \delta(\mathbf{x}). \quad (23)
\end{aligned}$$

At the critical coupling for S-states  $\lambda_c = \pi^2$ , the relativistic Coulomb bound states have a size of order  $1/\sqrt{\lambda_c T_c}$  for  $\mu \approx \pi T_c$  [3], smaller than the electric and magnetic screening lengths (see below and also [3]). The spin-spin term is then of order

$$\frac{\pi^2 T_c}{3} \vec{S}_1 \cdot \vec{S}_2. \quad (24)$$

This causes a splitting between the spin-1 and spin-0 of about  $\pi^2 T_c/3 \approx \pi T_c$ . However, since the coupling is rather large, the issue is calling for a strong coupling reassessment of the spin-induced interactions.

**Potentials in strong coupling.** In strong coupling a resummation of the ladders is warranted as described above. The kernel can be expanded in powers of relative time  $S - T$  to second order, yielding the oscillator-type Schrodinger equation. The result is the following potential

$$\begin{aligned}
\mathbf{V}_{\text{ladd}12}(\mathbf{x}) &= -\frac{\sqrt{\lambda}}{\pi |\mathbf{x}|} \left[ \left( 1 - \frac{\vec{p}_1 \cdot \vec{p}_2}{\mu^2} \right) \right. \\
& + \frac{1}{\mu^2 |\mathbf{x}|^2} (\vec{\sigma}_2 \cdot (\vec{x}_{21} \times \vec{p}_1) + 1 \leftrightarrow 2) \\
& \left. + \frac{1}{\mu^2 |\mathbf{x}|^2} \left( \frac{1}{3} \vec{\sigma}_1 \cdot \vec{\sigma}_2 - 2\sigma_{T12} \right) \right]^{1/2}. \quad (25)
\end{aligned}$$

where the Coulomb, Amper, spin-spin and spin-orbit terms all enter together into the common frequency of the effective oscillator.

**Corrections to Coulomb bound states** due to spin-spin and spin-orbit terms discussed above are easy to estimate only for weakly bound states, for which the non-relativistic limit  $\mu \rightarrow m$  can be used. In general, the quantity  $\mu = m\gamma$ , or the ‘‘relativistic kinetic energy’’ of the particle as we will refer to it, is only defined precisely for a given path.

A particular quantum state can be viewed as a sum of many paths, so one should average the potential over them. It is in general a nontrivial problem we are not trying to solve in this work. We will however provide a semiclassical estimate, substituting the kinetic energy  $\mu$  by the total energy minus the potential  $E - V$ . Semiclassically, the total energy  $E$  is the sum of kinetic ones plus a potential

$$E = \sqrt{p_1^2 + m^2} + \sqrt{p_2^2 + m^2} + V = 2\mu + V \quad (26)$$

and thus the variations of  $\mu$  are opposite to those of  $V$  as the particle mover from one position to the next.

This clarifies the following paradox. Naively, if one would think of  $\mu$  as a constant, the factors of  $1/x\mu$  in spin-spin and spin-orbit terms appear to signal their dominance at small distances. This is not so if it is understood as  $\mu \rightarrow E - V$ , which at small distances is dominated by the Coulomb potential. Therefore, in the strong coupling, one finds that at small distances it is in fact suppressed  $1/(\mu x) \approx 1/\sqrt{\lambda} \ll 1$ .

In strong coupling the angular momentum is of order  $\sqrt{\lambda}$ . Thus, the spin-orbit coupling is of order  $1/\sqrt{\lambda}$  while the spin-spin coupling is of order  $1/\lambda$ , both of which are subleading in the strong coupling limit.

This justifies *a posteriori* the use of the Coulomb orbit in the determination of  $\mu$  and shows that the results of [3] are left unaffected by spin effects.

As an example, let us consider the case of ultrarelativistic strongly coupled S-states  $|p_1| = |p_2| = \mu$ . The interaction in this case reads is

$$\mathbf{V}_{\text{ladd } 12}^{L=0}(\mathbf{x}) = -\frac{\sqrt{\lambda}}{\pi|\mathbf{x}|} \left[ 1 + 1 + \frac{4\pi^2}{3\lambda} \vec{S}_1 \cdot \vec{S}_2 \right]^{1/2}, \quad (27)$$

To leading order in strong coupling, the spin-0 and spin-1 S-states are actually degenerate. Note also, that the sign of the spin-spin term is now opposite to the Breit-Fermi one.

**Effects of screening at finite-temperature.** The above results apply to an unscreened interaction. In the presence of screening the Coulomb and spin induced interactions are modified since the electric and magnetic interaction are screened as discussed in [3]. In the ladder approximation and weak coupling, the electric effects are Debye screened at distances of the order of the inverse Debye length  $1/m_D \approx 1/\sqrt{\lambda T}$ , while the magnetic effects are screened at distances of the order of the inverse magnetic length  $1/m_M \approx 1/\lambda T$ . The magnetic length is much larger than the electric length in weak coupling, causing the magnetic effects to be dominant at asymptotically large temperatures as in QCD. As a result, magnetically bound Coulomb states may form, see e.g. discussion of the so called “screened masses” in [15] and more recent discussion of Cooper pair formation and color superconductivity [16]. In strong coupling and in the ladder approximation, the magnetism is there together with the Coulomb term in the form of Ampere’s term, while the spin-induced effects are kinematically suppressed as shown above. String arguments suggest that the electric and magnetic screening are comparable in strong coupling, and of order  $1/\pi T$  [3]. We have used the latter point of view at  $T_c$  in QCD. This point deserves further investigation.

**Summary and discussion.** Using the ladder re-

summation in strong coupling, we have assessed the spin-spin and spin-orbit potentials between two external “spinning” fermion paths. The results in matter follow readily from the screened potentials discussed in [3]. These results can be checked using the ADS/CFT correspondence from the large time asymptotics of the correlator (6) in strong coupling and large  $N$ .

In strongly coupled  $\mathcal{N} = 4$  SYM at finite temperature, there are deeply bound Coulomb states with orbital angular momentum  $\sqrt{\lambda}$ , with the total energy  $E \sim T$  and independent on  $\lambda$ , with sizes of the order  $1/\sqrt{\lambda T}$ . These states are bound by ordinary Coulomb (plus Ampere’s) law: we have now shown that for them the spin-orbit and spin-spin interactions are subleading effects.

These findings are important for evaluation of related effects in QCD at  $T = (1 - 3)T_c$  in which it undergoes a transition into an intermediately coupled Coulomb phase. The pertinent splitting is the  $\rho - \pi$  meson splitting across the region, a very important issue for a number of signals at RHIC, such as the dilepton emission [1].

As we shown above, if one uses the weak coupling result – the standard Breit-Fermi interaction – at the critical (for the S-states) coupling  $\lambda_c = \pi^2$ , it yields a large splitting between the spin-0 and spin-1 states of order  $\pi T_c$ . However our arguments above imply a kinematical suppression by relativistic factors, on top of which is the flipped sign of the spin-spin coefficient, from weak to strong coupling. It all shows that the issue should need a special careful examination, both by analytic means and on the lattice.

## Acknowledgments

We thank Gerry Brown for discussions. This work was supported in parts by the US-DOE grant DE-FG-88ER40388.

- 
- [1] E. V. Shuryak, *Phys.Rep.* 61 (1980) 71
  - [2] I. Zahed, ‘Light relativistic bound states in high temperature QCD’, Ed. H. Ezawa, T. Arimitsu and Y. Hashimoto, (1991) North Holland, p. 357, and references therein.
  - [3] E. V. Shuryak and I. Zahed, [hep-ph/0307267](#); [hep-th/0308073](#).
  - [4] J. Maldacena, *Adv. Theor. Math. Phys.* **2** (1998) 231, [hep-th/9711200](#); *Phys. Rev.* **80** (1998) 4859, [hep-th/9803002](#) and references therein.
  - [5] S.-J. Rey and J.-T. Yee, *Eur. Phys. J.* **C22** (2001) 379, [hep-th/9803001](#).
  - [6] M. Rho, S.J. Sin and I. Zahed, *Phys. Lett.* B466 (1999) 199, [hep-th/9907126](#)

- [7] R. A. Janik and R. Peschanski, Nucl. Phys. **B565** (2000) 193; [hep-th/9907177](#)
- [8] J. Polchinski and M.J. Strassler, Phys. Rev. Lett. **88** (2002) 031601, [hep-th/0109174](#).
- [9] G.T. Horowitz and A. Strominger, Nucl. Phys. **B360** (1991) 197. S.S. Gubser, I.R. Klebanov and A.A. Tseytlin, Nucl. Phys. **B534** (1998) 202; C.P. Burgess, N.R. Constable, R.C. Myers, JHEP **1999** 9908, C. Kim and S.J. Rey, Nucl. Phys. **B564** (2000) 430.
- [10] S.-J. Rey, S. Theisen and J.-T. Yee, Nucl. Phys. **B527** (1998) 171, [hep-th/9803135](#)
- [11] G. Policastro, D. T. Son and A. O. Starinets, Phys. Rev. Lett. **87** (2001) 081601.
- [12] A. O. Starinets, Phys. Rev. D **66** (2002) 124013, [hep-th/0207133](#).
- [13] G. W. Semenoff and K. Zarembo, Nucl. Phys. Proc. Suppl. **108**, 106 (2002), [hep-th/0202156](#).
- [14] Y. Simonov, [hep-ph/0203059](#), and references therein.
- [15] T.H. Hansson and I. Zahed, Nucl. Phys. **B374** (1992) 277; F.V. Koch, E.S. Shuryak, G.E Brown and A. Jackson, Phys. Rev. **D46** (1992) 3169; T.H. Hansson, M. Sporre and I. Zahed, Nucl. Phys. **B427** (1994) 545.
- [16] D. T. Son, Phys. Rev. **D59**, 094019 (1999) [[hep-ph/9812287](#)].
- [17] A. Strominger, Phys. Lett. **B101** (1981) 271; A.M. Polyakov, Mod. Phys. Lett. **A3** (1988) 325.